

High-Precision Construction of Colloidal Superstructures through Cucurbit[n]Urils-Mediated Self-Assembly

Huimin Xie, Chengzhi Guo, Shuyu Zhu, Jing Yan, Yuwen Zhang,* and Yang Lan*

In the past decades, colloid research has experienced significant growth across various scientific disciplines. This review explores recent advancements in the design and fabrication of cucurbit[n]urils (CB[n])-mediated self-assembly for colloids with advanced structures. CB[n], a class of macrocyclic molecules known for their distinctive host–guest interactions, plays a crucial role in synthesizing colloidal superstructures due to their ability to form stable complexes with a wide range of guest molecules. This review provides a comprehensive summary of recent advances in CB[n]-mediated self-assembly strategies for constructing diverse colloidal architectures. These assemblies are systematically categorized into distinct types, including colloidal clusters, 1D colloidal chains, raspberry-like colloids, core–shell colloids, and colloidosomes. While the primary emphasis is placed on construction methodologies, the potential applications of these superstructures are also briefly highlighted in areas such as drug delivery, catalysis, and sensing, to illustrate their relevance in the development of functional materials. By examining the synthesis methods and potential applications, this review underscores the versatility and adaptability of CB[n]-mediated colloidal systems and their potential to drive future innovations in colloid science.

1. Introduction

Colloids and their assemblies, renowned for their small size, customizable structures, and adjustable surface chemistry, are highly desirable for a diverse range of applications, including electronics, energy storage, and biomedical engineering.^[1–3] Recent advances in this field highlight the development of sophisticated colloidal structures based on geometric and morphological considerations to enhance material functionalities. Key innovations encompass the fabrication of colloidal superstructures such as colloidal clusters,^[4] one-dimensional (1D) colloidal chains,^[5] raspberry-like colloids,^[6] core–shell particles,^[7] and colloidosomes.^[8] These intricate colloidal configurations exhibit unique properties that expand their applicability. For instance, the exceptional durability of raspberry-shaped colloids in salting-out phenomena highlights their significance in aqueous environments with elevated salinity levels.^[6] These properties establish their particular significance in sectors like pharmaceutical delivery systems and oil extraction.

The high-precision construction of colloidal superstructures primarily involves chemical, physical, and supramolecular approaches. Chemical methodologies, such as sol–gel processes^[9] and emulsion polymerization,^[10] have significantly contributed to the production of colloids by facilitating control over particle size and morphology. However, developing effective formulation remains challenging and often requires extensive experimentation.^[11–15] Physical methods, such as physical vapor deposition,^[16] play a significant role in the generation of colloidal superstructures. Nevertheless, they encounter difficulties in scaling up for high particle throughput and ensuring uniformity in large quantities.^[17,18] To address these challenges, supramolecular methods have emerged as promising alternatives, leveraging non-covalent interactions, such as host–guest interactions and self-assembly processes, to create colloidal structures with precise control over size, morphology, and composition. This paradigm offers solutions that address the limitations of chemical and physical methods in producing colloidal superstructures.^[17,19]

Cucurbit[n]urils, abbreviated as CB[n]s, represent a category of macrocyclic compounds composed of glycoluril units interconnected by methylene bridges (Figure 1A).^[20] The variable “n” represents the number of glycoluril units in CB[n], which

H. Xie, S. Zhu, Y. Zhang
College of Chemistry and Chemical Engineering
Lanzhou University
Lanzhou, Gansu 730000, China
E-mail: zhangyw@lzu.edu.cn

C. Guo, Y. Lan
Centre for Nature-Inspired Engineering
Department of Chemical Engineering
University College London
London WC1E 7JE, UK
E-mail: yang.lan@ucl.ac.uk

J. Yan
Department of Veterinary Medicine
University of Cambridge
Cambridge CB3 0ES, UK

The ORCID identification number(s) for the author(s) of this article can be found under <https://doi.org/10.1002/macp.202500107>

© 2025 The Author(s). Macromolecular Chemistry and Physics published by Wiley-VCH GmbH. This is an open access article under the terms of the [Creative Commons Attribution](#) License, which permits use, distribution and reproduction in any medium, provided the original work is properly cited.

DOI: 10.1002/macp.202500107

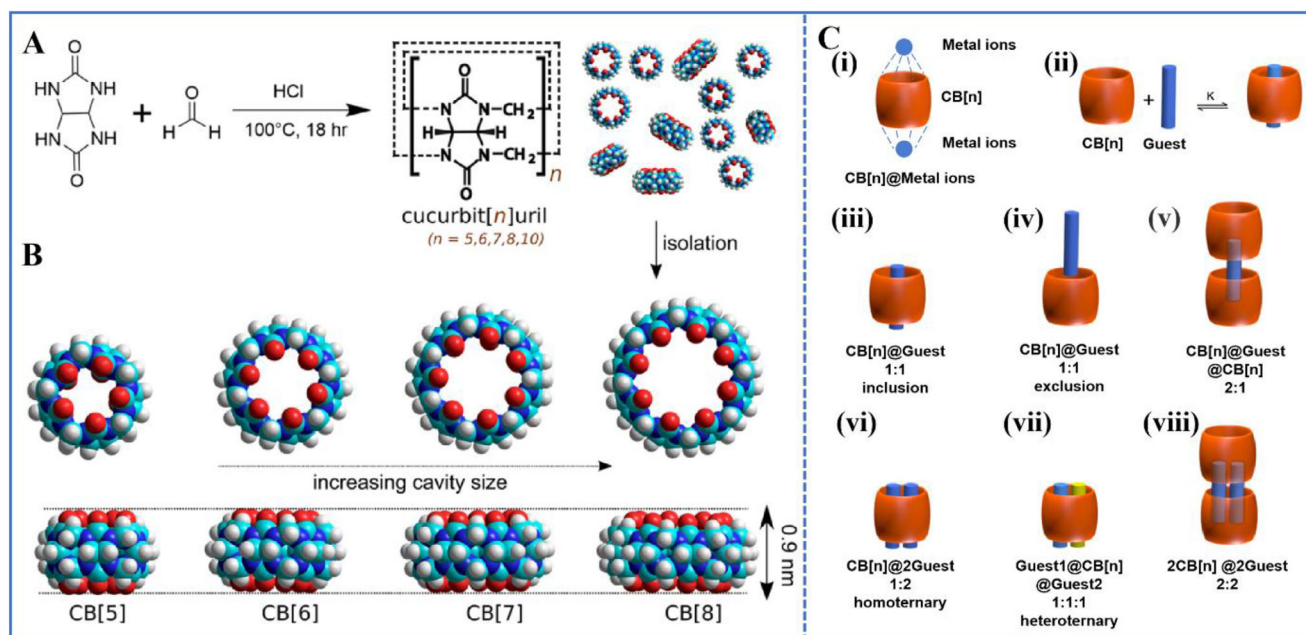


Figure 1. A) Synthesis of cucurbit[n]uril (CB[n]) through the condensation reaction of glycoluril and formaldehyde. B) Space-filling models of CB[5]–CB[8], illustrating the progressive enlargement yet consistent height of the CB[n] macrocycles. C) Schematic representation of CB[n]-assisted host–guest complexation modes.^[20] Reproduced with permission from ref. [20] copyright 2015, American Chemical Society.

dictates the size and capability of the macrocyclic framework. Freeman et al.^[21] pioneering the work in 1981 led to the synthesis of CB[6] through the condensation reaction of glycoluril and formaldehyde. This first cucurbit[n]uril variant, CB[6] features six glycoluril units and twelve methylene bridges, with a pumpkin-like shape that formed the basis of the cucurbit[n]uril family. Since then, the cucurbit[n]uril family has grown to include CB[5], CB[7], CB[8], CB[10], and CB[13] each distinguished by the number of glycoluril units.^[22–25] Despite differences in size, all CB[n] variants share a consistent height of 0.91 nm (Figure 1B), giving them a toroidal shape that boosts their strength and stability, making them robust hosts for selective guest molecules via distinct binding sites and configurations.^[21]

The study highlights that CB[n] possesses two distinct binding sites for guest molecules. The first, located at the carbonyl-fringed portals, exhibits an inherent negative charge that attracts cations through ion–dipole interactions, as illustrated in Figure 1C-i.^[26] The second binding site of CB[n] is the inner cavity, characterized by its hydrophobic nature, which enables the encapsulation of specific compounds (Figure 1C-ii). Compatibility between CB[n] and guest molecules is often assessed through packing coefficients,^[27,28] providing insights into the binding affinity and selectivity of the CB[n]–guest complex.^[26] The cavity sizes of CB[n] compounds increase progressively from CB[5] to CB[8], influencing their encapsulation capabilities and determining the mode of encapsulation. Specifically, CB[5], CB[6], and CB[7] typically host a single guest molecule within their cavities, forming either binary complexes (CB[n]@Guest 1:1, Figure 1C-iii,iv) or ternary complexes comprising two CB[n]s and one guest molecule (CB[n]@Guest@CB[n] 2:1, Figure 1C-v).^[28,29] CB[5], the smallest member, binds cations like NH_4^+ and Pb^{2+} at its entrances, while its cavity can accommodate only small

gas molecules such as N_2 .^[30–32] CB[6], with a larger cavity, forms stable binary complexes (CB[n]@Guest 1:1, Figure 1C-iii) with protonated diaminoalkanes and aromatic amines through ion–dipole interactions.^[33] CB[7], specialized for larger guests, engages in binary complexes (CB[n]@Guest 1:1, Figure 1C-iii) with entities such as protonated adamantylamine (ADA) and methyl viologen (MV) dication.^[34,35] CB[8] is large enough to simultaneously accommodate two guest molecules inside its cavity, leading to the formation of either homoternary complexes with two identical guest molecules (CB[n]@2Guest 1:2, Figure 1C-vi) or heteroternary complexes with two distinct guest molecules (Guest1@CB[n]@Guest2 1:1:1, Figure 1C-vii).^[36] In some cases, CB[8] can also form four-molecule complexes (2CB[n]@2Guest 2:2) as shown in Figure 1C-viii.^[37,38] For example, CB[8] forms binary complexes (CB[n]@Guest 1:1) with electron-deficient guests such as MV and can sequentially bind electron-rich guests such as azobenzene (Azo), naphthalene (Np), phenylalanine, and tryptophan derivatives to form stable heteroternary complex (Guest1@CB[n]@Guest2 1:1:1). Additionally, CB[8] can also form homoternary complexes (CB[n]@2Guest 1:2) under specific conditions, such as when guest molecules possess a positively charged site or when guest molecules such as viologen dications (MV^{2+}) undergo one-electron reduction to the radical cation ($\text{MV}^{\bullet+}$).^[39]

For a better understanding of CB[n]’s molecular recognition properties, readers are encouraged to refer to comprehensive reviews on this topic.^[20,28,40–42] By leveraging the selective binding properties and distinctive binding configurations of CB[n] with guest molecules, it is possible to effectively control the formation and arrangement of colloidal particles, leading to the formation of colloidal superstructures. This review highlights recent developments underscoring the pivotal role of CB[n] in the synthesis

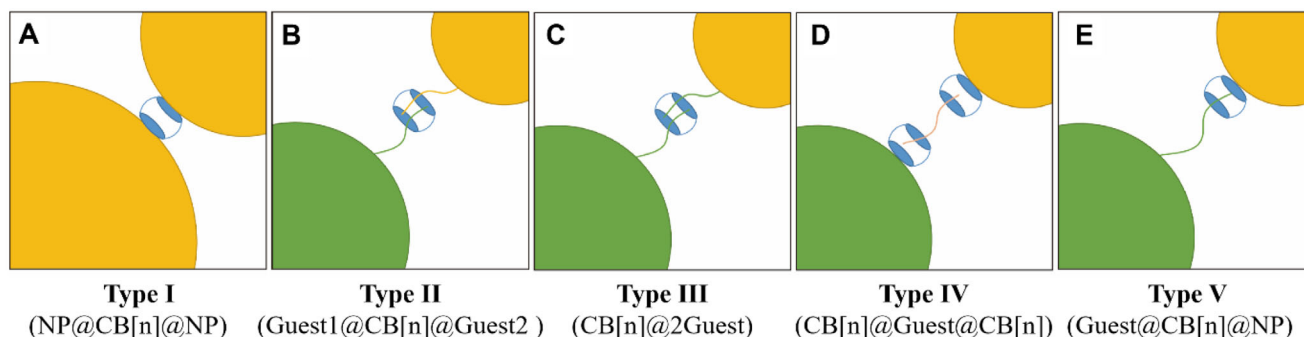


Figure 2. Schematic representation of CB[n]-facilitated host-guest self-assembly of colloids. A) Type I: CB[n] portals directly capture two identical or different colloids, forming colloidal clusters or chains through the inherent affinity between CB[n] and metal nanoparticles. B) Type II: CB[n] is immobilized on two distinct colloids, and a linker molecule with dual guest functionalities mediates binary complex formation (CB[n]@Guest 1:1), enabling structured multi-colloid assemblies. C) Type III: Identical guest molecules on two colloids are bridged by CB[n], forming homoternary complexes (CB[n]@2Guest 1:2) for creating interconnected colloidal networks. D) Type IV: Distinct guest molecules on different colloids are linked by CB[8] through heteroternary complex formation (Guest1@CB[8]@Guest2 1:1:1), facilitating multi-component assemblies. E) Type V: A single type of CB[n] immobilized on one colloid interacts with guest-modified particles via binary complex formation (CB[n]@Guest 1:1), achieving simplified yet precise assembly.

and self-assembly of colloidal superstructures. It focuses on various construction techniques and demonstrates the transformative impact of CB[n]-mediated approaches on the design of advanced colloidal materials.

2. Colloidal Superstructures Constructed through CB[n]-Mediated Self-Assemblies

The unique binding properties of CB[n] support a variety of sophisticated strategies to facilitate the self-assembly of colloidal superstructures, capitalizing on their exceptional molecular recognition capabilities. The first and most successful approach utilizes CB[n] macrocycles to capture two identical or different types of colloids by utilizing the portals of the CB[n] for self-assembly (Type I, Figure 2A).^[43] This approach exploits the inherent affinity between the carbonyl portals of CB[n] and metal nanoparticles, thereby enabling the creation of sophisticated colloidal structures, such as colloidal clusters and chains, through precise alignment and binding. This technique proves particularly valuable in the construction of metal nanoparticle-based structures. Another successful approach involves immobilizing CB[n] molecules onto two distinct types of colloidal particles (Type II, Figure 2B).^[44] Subsequently, a linker molecule, carrying two guest molecules, is utilized to engage with the CB[n] units on each category of colloid via the formation of binary complexes (CB[n]@Guest 1:1). This interaction promotes the formation of intricate, highly structured configurations by the specific bonding guest molecules to CB[n] units, achieving precise spatial arrangement and incorporation of multiple colloidal varieties into a cohesive structure. A third strategy involves the functionalization of identical guest molecules on two distinct types of colloids (Type III, Figure 2C).^[45]

Here, CB[n], normally CB[8], acts as a “handcuff” or bridge, to facilitate the assembly of these colloids by creating a homoternary complex of CB[n]@2Guest 1:2. Within this arrangement, a single CB[n] molecule connects two colloidal particles, both containing identical guest molecules, thereby facilitating the creation of a complex colloidal network with superior structural integrity. Similarly, it is also effective to employ the functionalization of

different guest molecules on two distinct types of colloids, with CB[8] acting as a linker to mediate the assembly through the formation of heteroternary complexes of Guest1@CB[n]@Guest2 1:1:1 for the formation of colloidal superstructures (Type IV, Figure 2D).^[46] In this approach, each type of colloid is functionalized with a unique guest molecule, and a single CB[8] macrocycle coordinates the simultaneous interaction with these guest molecules. This creates a three-component assembly where the CB[8] facilitates the precise alignment and binding of the colloids, resulting in complex, multi-component structures. In addition, a more straightforward yet efficient approach entails immobilizing a single variety of CB[n] on a particular colloidal particle and modifying a distinct type of colloidal particle with guest molecules (Type V, Figure 2E).^[34] The assembly is accomplished by utilizing the CB[n] portal binding site and the formation of binary complexes (CB[n]@Guest 1:1), where a single CB[n] molecule attaches to one guest molecule on a different colloid. Overall, each of these methodologies leverages the distinctive binding characteristics of CB[n] to accomplish precise and refined self-assembly of colloidal systems, showcasing the adaptability and promise of CB[n] in the realm of colloidal science. The utilization of CB[n]-based mediation strategies for the self-assembly of various colloidal superstructures will be summarized in the upcoming instances. These illustrations will elucidate how each technique fosters the creation of particular colloidal architectures, emphasizing the adaptability of CB[n] in orchestrating colloidal superstructures.

2.1. Colloidal Clusters

Colloidal clusters are intricate assemblies of small particles that aggregate to form larger structures.^[4] These clusters consist of colloidal particles, usually within the nanometer to micrometer range. One important characteristic of colloidal clusters is the interactions between the particles comprising these clusters, which include van der Waals forces, electrostatic interactions, and covalent or ionic bonds.^[47,48] The complex interplay of these forces confers unique structural and functional properties upon the

clusters, making them highly relevant in multiple scientific and technological domains. Another key characteristic of colloidal clusters is the variable number of small particles they contain, typically ranging from two (dimers) to several hundred, with reduced dimensionality often resulting in phenomena absent in bulk materials.^[49,50] These characteristics render colloidal clusters particularly valuable in materials science, where they contribute to the development of novel composite materials used in sensing, drug delivery, and catalysts. Colloidal clusters can form through various mechanisms, including self-assembly, chemical reactions, and physical aggregation.^[48,51,52] Understanding the formation and properties of colloidal clusters remains a vibrant area of research, with ongoing studies revealing new applications and providing deeper insights into the fundamental science of these intricate structures.

2.1.1. Formation of Inorganic Nanoparticle Clusters

Inorganic nanoparticle clusters are highly organized assemblies of individual nanoparticles that exhibit unique physical and chemical properties distinct from their constituent components. These clusters are known for their enhanced optical, electronic, and catalytic behaviors, making them valuable in fields such as nanomedicine, catalysis, and environmental sensing. Conventional methods for assembling such clusters often rely on electrostatic interactions, ligand-mediated stabilization, or chemical cross-linking, which can lack precision and dynamic tunability. The use of CB[n] macrocycles introduces a novel strategy for self-assembling inorganic nanoparticle clusters through host–guest interactions at the molecular level. CB[n] acts as a molecular linker, leveraging its carbonyl portals to interact selectively with nanoparticles, facilitating precise spatial arrangements and forming stable, responsive structures. In a pioneering example, Lee's marked the first use of CB[n] macrocycles in mediating the self-assembly of colloidal particles, creating dynamic and responsive colloidal clusters.^[43] In this study, gold nanoparticles (AuNPs) were assembled into clusters through supermolecular interactions between the carbonyl portals of CB[5] and AuNPs (Type I, Figure 2A). The formation process involved reducing tetrachloroauric acid (HAuCl₄) with sodium borohydride (NaBH₄) in the presence of CB[5], which promoted the creation of AuNP clusters either singly or doubly capped by CB[5] at its carbonyl portals (Figure 3A-i). By varying the ratio of CB[5] to the gold precursor, Lee demonstrated control over the cluster size and configuration, with increased CB[5] content transforming linear colloidal chains to 3D clusters of reduced size. Transmission electron microscopy (TEM, Figure 3A-ii–vii) further highlighted the precise tunability of cluster sizes based on CB[5] concentration. This research introduces an innovative approach to stabilizing metal nanoparticles using CB[5] as a capping agent, forming dynamic colloidal clusters with potential applications in catalysis and sensing. It makes an important step toward exploring CB[n]-facilitated self-assembly for the creation of colloidal superstructures.

Building on Lee's pioneering demonstration of CB[n]-mediated colloidal assembly, the field has rapidly shifted from mere structural proofs of concept to the exploration of highly tunable, function-oriented nanostructures. At the heart of this evolution lies the capacity of CB[n] macrocycles to exert sub-

nanometer control over nanoparticle spatial organization while simultaneously providing selective molecular recognition. This dual functionality has opened avenues for innovative plasmonic and sensing applications, transforming static clusters into dynamic, responsive architectures. A significant advance in exploiting these assemblies for plasmonic enhancement emerged with Taylor et al.^[53] who leveraged CB[5] and CB[7] to establish sub-nanometer gaps in AuNP clusters (Figure 3B). Such precise gap control, intrinsically tied to the CB[n] portal geometry, was crucial for creating uniform “hot spots” capable of reliable and reproducible surface-enhanced Raman spectroscopy (SERS). This strategy highlighted the capacity to integrate molecular-level sensing and materials assembly into a single supramolecular platform.

The versatility of CB[n]-based assemblies became further evident when Teng et al.^[54] targeted environmental applications. By employing CB[8] to create 1 nm interparticle separations, they engineered hotspots ideal for detecting endocrine-disrupting compounds such as estrone (E1), bisphenol A (BPA), and diethylstilbestrol (DES) (Figure 4A). These studies underscored the importance of exploiting host–guest chemistry not just for controlling nanoparticle arrangement, but also for selectively concentrating target analytes within plasmonic junctions. This approach demonstrated how subtle tweaks, such as matching the size and binding affinities of CB[8] to specific pollutants, can translate into enhanced sensitivity and selectivity, paving the way for real-world monitoring of water contamination and other environmental challenges. In parallel, Davison et al.^[55] expanded the scope of CB[n]-mediated designs by introducing computational methods and numerical simulations to optimize cluster formation and plasmonic performance. Their work showcased the fine-tuning of nanoparticle geometry and gap distances under 1 nm through CB[7] bridging, culminating in ultrasensitive, single-molecule-level SERS (Figure 4B). By systematically integrating supramolecular chemistry, computational design, and advanced nanoparticle synthesis, this research points to a future where CB[n]-based assemblies are tailored with near-atomic precision for analytical, diagnostic, and other high-value applications.

Collectively, these follow-up works illustrate a vibrant progression in CB[n]-mediated nanoparticle cluster engineering, moving from foundational self-assembly principles to sophisticated functional systems. Through precise gap control, selective host–guest interactions, and adaptability to various analytes, CB[n] macrocycles have proven themselves integral to designing next-generation plasmonic materials. As such, they embody a powerful strategy for bridging the gap between fundamental nanochemistry and practical applications in environmental sensing, diagnostics, and beyond.

2.1.2. Formation of Polymeric Colloidal Clusters

Beyond leveraging the carbonyl portals of CB[n] to directly coordinate with metal nanoparticle surfaces (Type I, Figure 2A), a parallel strategy uses CB[8]-mediated heteroternary complexation (Type II, Figure 2B) to assemble colloidal particles into sophisticated polymeric architectures. In this approach, CB[8] acts as a supramolecular “bridge” between two complementary functional groups, which are often placed on different colloidal particles,

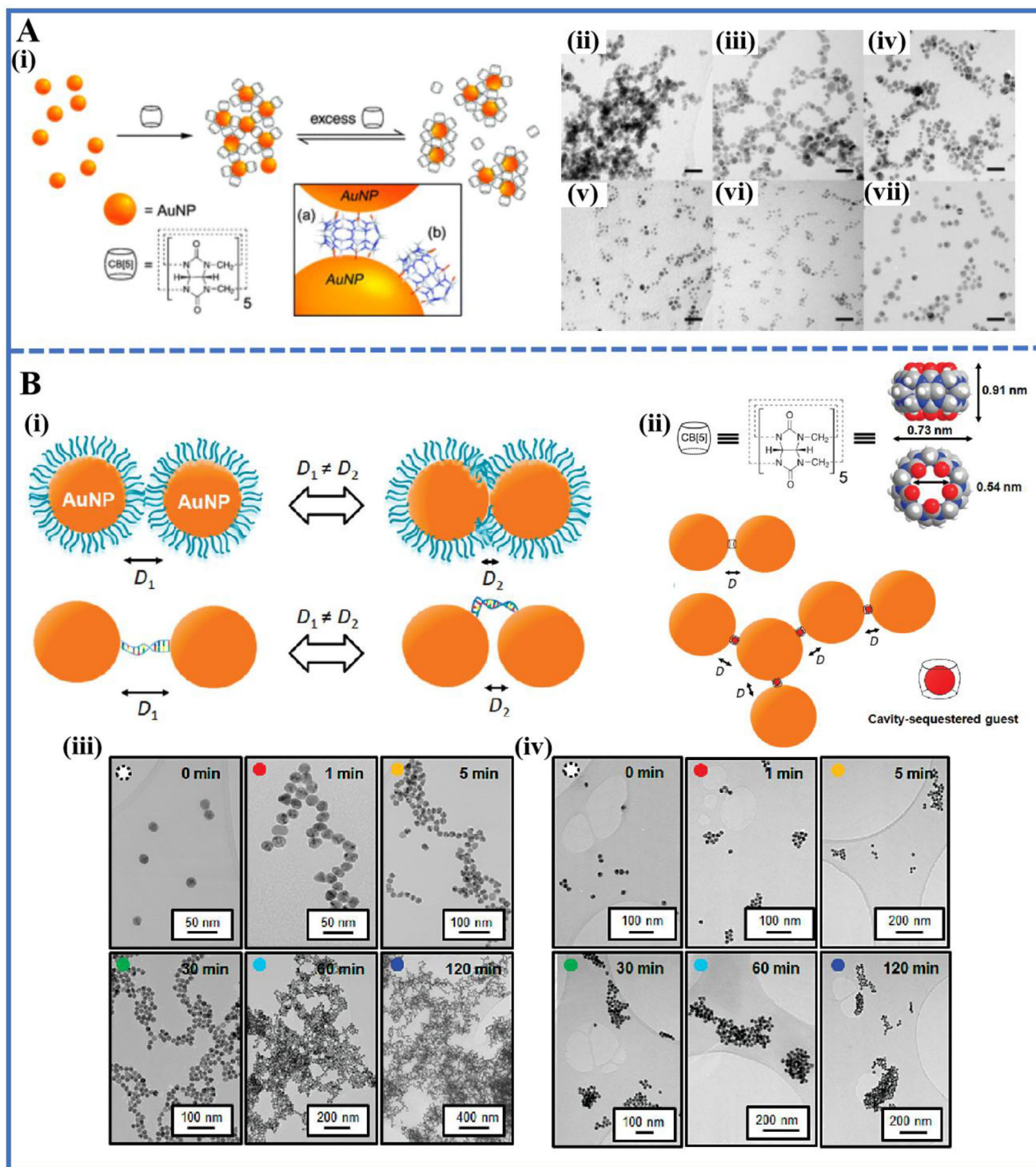
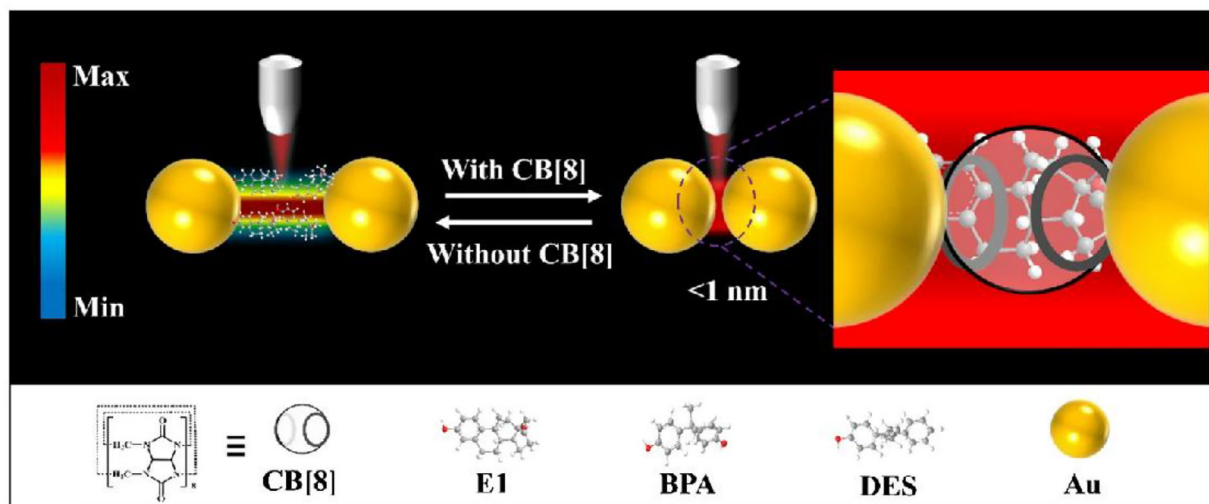
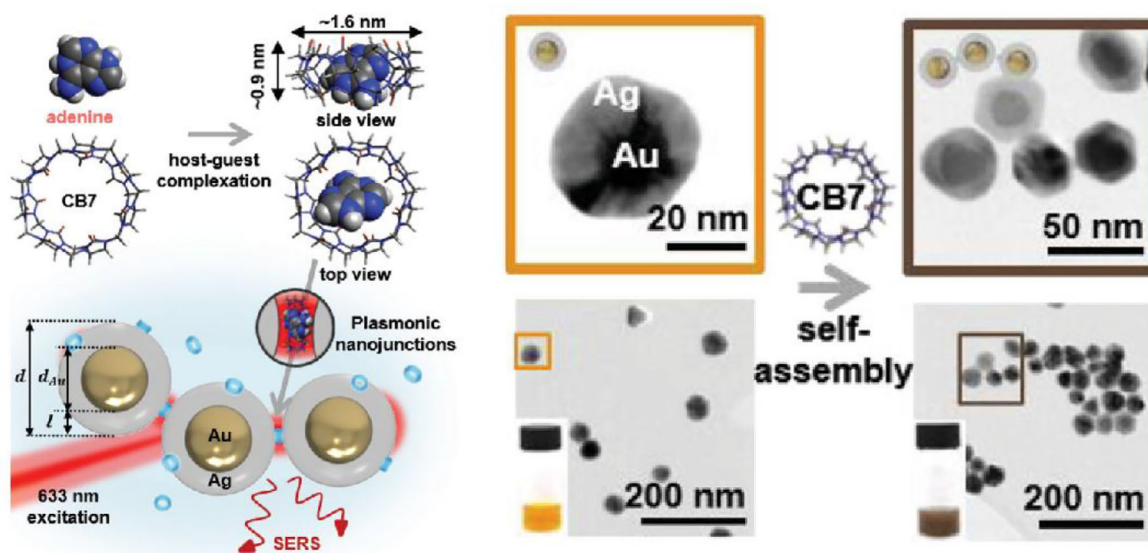


Figure 3. A) i) Formation of AuNP clusters mediated by CB[5] in aqueous media, with inset showing CB[5] doubly and singly capped by AuNPs. TEM images depict of AuNP clusters at varying CB[5]/Au ratios: ii) 0, iii) 0.1, iv) 0.2, v) 0.5, vi) 1, and vii) from 0 to 1 by addition of CB[5] after the reduction. Scale bar: 20 nm.^[43] Reproduced with permission from ref. [43] copyright 2010, The Royal Society of Chemistry. B) i) Current strategies for generating AuNP clusters coagulation with inconsistent and uncontrollable interparticle spacing. ii, iii, iv) AuNPs joined into either dimer or colloidal clusters by CB[5], with a portal-to-portal separation rigidly fixed at 0.9 nm. TEM images show representative aggregation products at specific time points, with variations in topology corresponding to the DLCA (m) and RLCA (n) regimes.^[53] Reproduced with permission from ref. [53] copyright 2011, American Chemical Society.

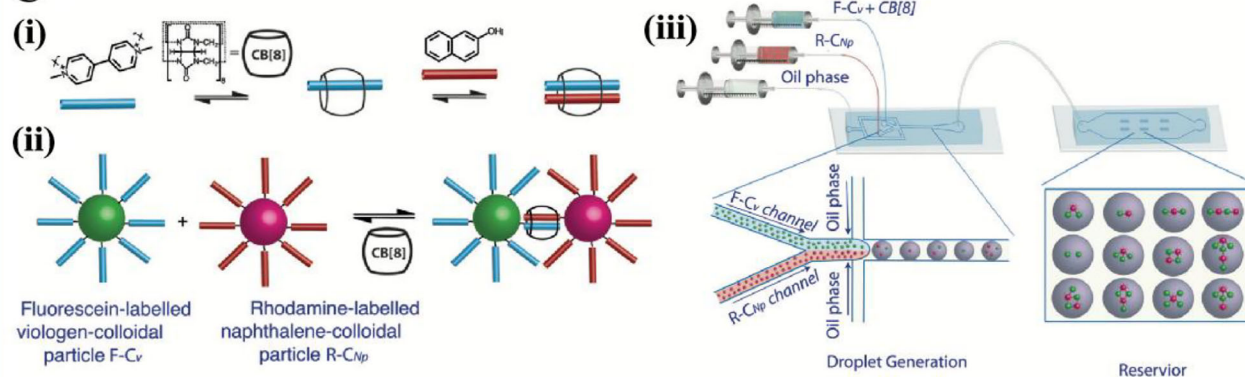
A



B



C



thus enabling the controlled organization of multiple building blocks into stable, higher-order structures.

A striking demonstration of this concept comes from the work of Xu et al.^[56] who employed microfluidic droplets as miniature reaction vessels to guide the assembly of polystyrene colloids functionalized with MV and Np (Figure 4C). By introducing these functionalized colloids into microdroplets in the presence of CB[8], they formed heteroternary complexes (MV@CB[8]@Np) that drove the precise clustering of colloids. This microfluidic setting allowed for fine-tuning of the colloidal concentration, yielding diverse and well-defined assemblies, including Janus particles, linear chains, and more complex square and pyramidal geometries. By capitalizing on the Poisson distribution of colloids within each droplet, the researchers achieved predictable control over both the number of particles per cluster and the resulting structural complexity.

2.2. One-Directional (1D) Colloidal Chains

1D colloidal chains represent a distinct class of nanostructures in which particles are arranged in elongated, linear configurations.^[5] These chains are characterized by their elongated structure, which results from the specific interactions among the constituent particles. The mechanical, optical, and electronic properties of colloidal chains depend on the alignment and proximity of the particles within them. A distinctive feature of 1D colloidal chains is their ability to exhibit anisotropic properties due to their linear structure.^[57] This reduced dimensionality imparts anisotropic behaviors that can be strategically exploited in photonics, electronics, and sensing, where directional transport and field enhancement are crucial.^[58,59] While external fields and templating have traditionally been used to create such linear assemblies,^[60] recent research has highlighted the unique capabilities of CB[n] supramolecular chemistry to drive precise, dynamic chain formation.

2.2.1. Formation of 1D Chains with Nanoparticles

Inspired by the formation of AuNP clusters through supramolecular interactions between the carbonyl portals of CB[n] and AuNPs (Type I, Figure 2A), Hüsken et al.^[61] investigated the preparation of 1D colloidal chains via the electrokinetic assembly of nanoparticles, with CB[7] controlling the subnanometer junctions between AuNPs (Figure 5A). By applying an electric field across a nanoporous membrane, they orchestrated the directional flow of CB[7] and AuNPs to create consistent 0.91 nm junctions. This level of sub-nanometer control is a hallmark of CB[n]-mediated assemblies, with the electrokinetic setup enabling fine-tuning of chain formation through voltage, reactant ratios, and

temperature. Consequently, Hüsken's approach offers a potent demonstration of how supramolecular recognition can be harnessed under dynamic, field-driven conditions to yield ordered 1D nanostructures.

2.2.2. Formation of Colloidal Chains with Nanorods

In parallel, Jones et al.^[44] explored the assembly of gold nanorods (AuNRs) into linear arrays using CB[8] host-guest interactions (Figure 5B). By functionalizing AuNRs ends with MV and employing telechelic linkers featuring Np, the authors achieved end-to-end alignment governed by a heteroternary complex (MV@CB[n]@Np). This system allowed for controlled end-to-end self-assembly of AuNRs (Type II, Figure 2B). This supramolecular strategy underscores the precision with which CB[n] can drive linear architectures: altering linker length or rigidity dramatically impacted the assembly, shifting the system from orderly chains to disordered aggregates. Furthermore, the assembly was rendered switchable via competitive binding, demonstrating that CB[n]-mediated 1D chains can be made reversible and stimuli-responsive, which is a key attribute for sensors and reconfigurable nanomaterials.

Building upon this responsive framework, Xu et al.^[45] introduced pH-dependent host-guest interactions to enable reversible transitions between assembled and dispersed AuNRs states (Figure 5C). This was achieved through the formation of a homoternary complex, CB[n]@2guest 1:2, in an aqueous solution (Type III, Figure 2C). Harnessing a homoternary complex (CB[n]@2guest), the authors modulated the system's protonation state to toggle chain formation on and off, highlighting the adaptability of CB[n] chemistry for creating dynamic, "smart" colloidal chains. This approach not only enhances control over nanorod assemblies but also paves the way for responsive materials with potential applications in nanoswitches and on-demand release systems.

2.2.3. Formation of Colloidal Chains with Patchy Particles

Expanding beyond metallic nanoparticles, researchers have also exploited CB[n]-mediated host-guest interactions to guide 1D assembly of "patchy" colloids, which are particles featuring chemically distinct surface regions. Benyettou et al.^[46] pioneered a redox-responsive scheme in which CB[7]-functionalized anisotropic polystyrene particles formed colloidal chains through diphenyl viologen (DPV) bridging (Figure 6A), which is mediated by CB[n] host-guest interactions (Type IV, Figure 2B). This approach highlighted the selectivity of homoternary complexes (CB[7]@2DPV) in directing reversible 1D chain formation, showcasing the versatility of CB[n] chemistry even in polymer-based systems.

Figure 4. A) A schematic representation illustrates the ligation of AuNPs and the capture of estrogen using CB[8].^[54] Reproduced with permission from ref. [54] copyright 2023, Springer Vienna. B) Formation of CB[7]-Au@Ag NPs precision nano-junctions through host-guest interactions and self-assembly, with TEM images and solution photographs showing the aggregation of Au@Ag NPs following CB[7] addition. Microfluidic-assisted self-assembly of polystyrene colloids into structured clusters mediated by CB[8].^[55] Reproduced with permission from ref. [55] copyright 2023, Wiley-VCH. C) i) Formation process of a three-component heteroternary complex in water mediated by CB[8] (blue rods: MV²⁺ and red rods: Np moieties). ii) Schematic representation of the assembly of the heteroternary complex between CB[8] and colloidal particles functionalized with MV²⁺ and Np. iii) Formation of structured colloidal assemblies within a droplet-based microfluidic system.^[56] Reproduced with permission from ref. [56] copyright 2015, Wiley-VCH.

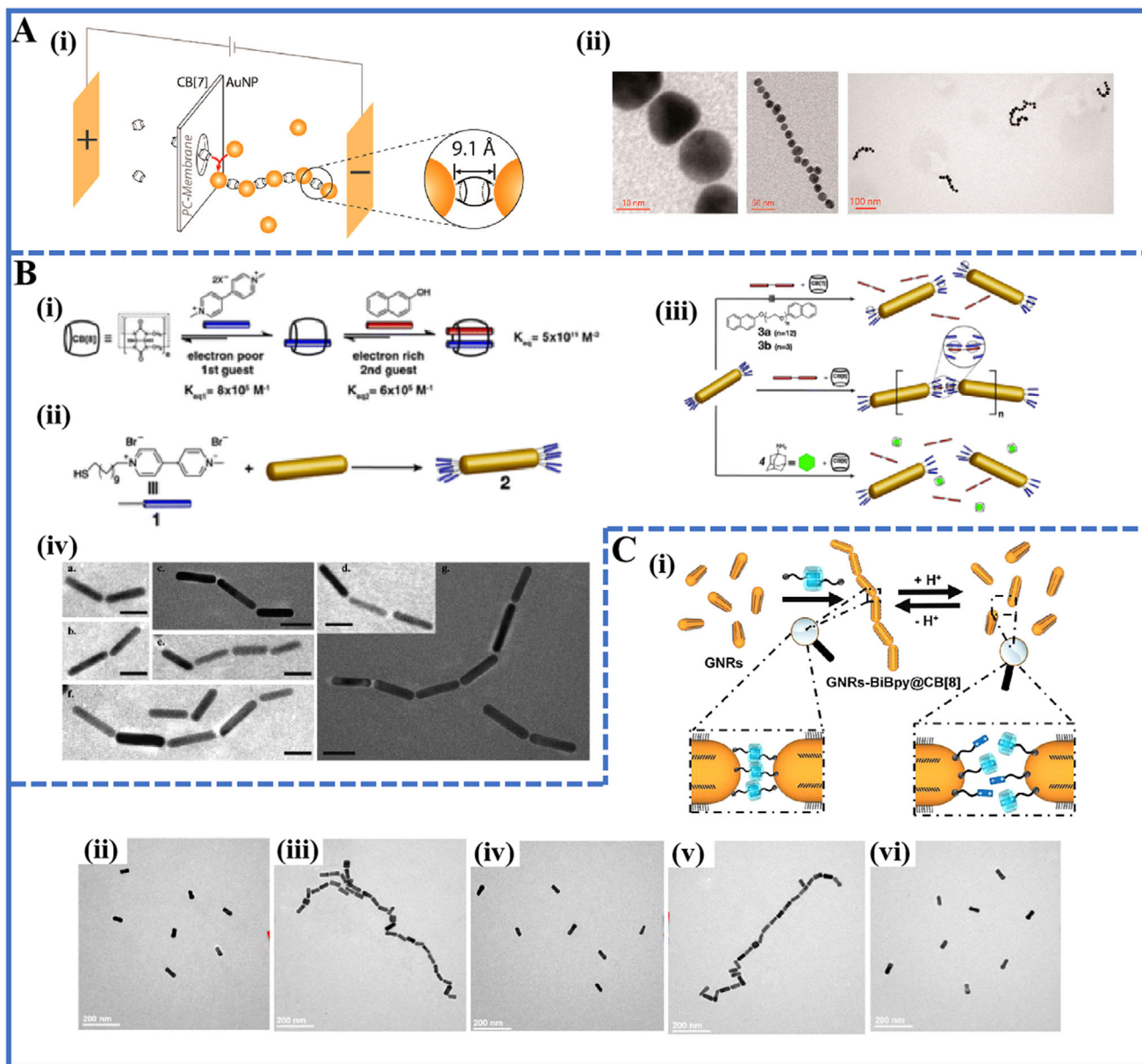


Figure 5. A) i) Formation of 1D chains of AuNPs and CB[7]. ii) TEM images of CB[7]-mediated AuNP chains at different magnifications.^[61] Reproduced with permission from ref. [61] copyright 2013, American Chemical Society. B) i) Formation of a heteroternary complex between MV, Np, and CB[8]. ii) Functionalization of AuNRs with MV moieties 1. iii) Addition of either di-Np linker (3a or 3b) with CB[7], with CB[8], or with CB[8] in the presence of 4. iv) TEM images depicting the alignment of AuNRs with di-Np linker 3b via CB[8] heteroternary complex formation. Scale bars, 25 nm.^[44] Reproduced with permission from ref. [44] copyright 2013, The Royal Society of Chemistry. C) i) Formation of pH-responsive assembly/disassembly processes of AuNR chains. TEM images showing ii) the original AuNRs, iii) end-to-end assembled AuNRs, iv) disassembled AuNRs after adjusting the solution pH to 2, v) end-to-end assembled AuNRs after adjusting the solution pH to 9, vi) disassembled AuNRs after adjusting the solution pH to 2 again.^[45] Reproduced with permission from ref. [45] copyright 2017, Elsevier Ltd.

Taking responsiveness a step further, Elacqua et al.^[62] incorporated light-triggered assembly and disassembly. By integrating azobenzene (Azo) and viologen (Vio) motifs within patchy colloids, they leveraged a heteroternary complex (Vio@CB[n]@Azo, Type II, Figure 2B) to generate 1D structures upon visible-light exposure (Figure 6B). UV irradiation caused *trans*–*cis* isomerization in the Azo group, breaking the complex and prompting disassembly while reversing the isomerization-restored linear as-

semblies. This photoregulated mechanism illustrated how multiple stimuli such as redox, pH, and light can be integrated into CB[n]-mediated colloidal chains, expanding the design space for sophisticated, adaptive materials.

In summary, these advances in 1D colloidal chains underscore the power of CB[n] host–guest chemistry to orchestrate precise, dynamic, and stimulus-responsive assemblies across a variety of particle types. Whether manipulating electrokinetic

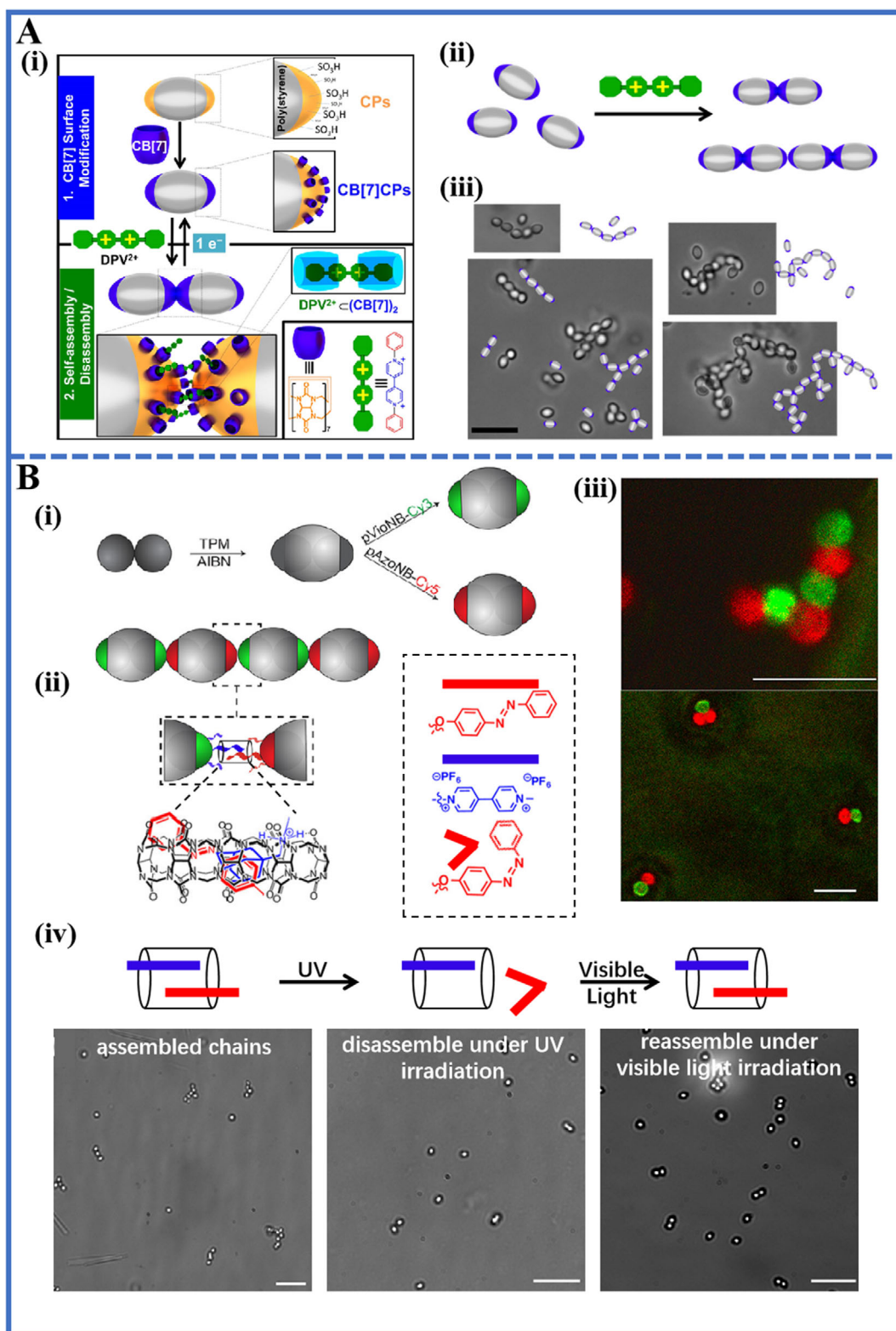


Figure 6. A) i) The scheme of a particle-particle junction shows a homoternary complex of CB[7]@2DPV 1:2 linking two particles. ii) Self-assembly of patchy particles induced by inclusion complex formation between DPV and CB[7]. iii) Microscopic images of chain-like structures consisting of multiple DPV-linked patchy particles. Scale bar, 4 μm.^[46] Reproduced with permission from ref. [46] copyright 2016, American Chemical Society. B) i) Fabrication of patchy particles from carboxylated poly(styrene) colloidal clusters. ii) Target host-guest-driven assembly mediated by CB[8]. iii) Confocal images of colloidal chains, Scale bar, 5 μm. iv) Bright-field microscopic images of assembled patchy colloids in the presence of CB[8]. Scale bar: 5 μm.^[62] Reproduced with permission from ref. [62] copyright 2017, American Chemical Society.

flows to create uniform junctions, guiding nanorods into well-aligned chains, or programming patchy colloids to respond to light and redox cues, researchers are increasingly leveraging CB[n]'s high specificity and tunable binding capacity to push the boundaries of colloidal self-assembly. These versatile strategies not only broaden the practical applications of linear colloidal structures in sensing, nanophotonics, and optoelectronics but also signal exciting new directions for designing adaptive, reconfigurable materials.

2.3. Raspberry-Like Colloidal Superstructures

Raspberry-like colloids are unique colloidal assemblies characterized by a core–corona structure that resembles the appearance of a raspberry.^[6] These colloids typically consist of a larger central core particle surrounded by a dense layer of smaller nanoparticles, creating a distinctive hierarchical arrangement. A notable feature of raspberry-like colloids is their ability to exhibit multifaceted properties that arise from both the core and corona components. This duality enables them highly responsive to external stimuli, enhancing their versatility across various applications.^[63–66] By precisely controlling the size and composition of the core and corona, researchers can tailor the physical and chemical properties of the colloids for specific purposes. Raspberry-like colloids are particularly valuable in advanced coatings and as hierarchical templates for fabricating complex structures, particularly in catalysis and drug delivery systems. As research continues to advance, these colloids open up exciting opportunities for innovation across various scientific and technological domains.

A key driver in realizing these intricate architectures has been the use of CB[n]-based host–guest chemistry, which enables precise, reversible, and stimulus-responsive assembly. Lan et al.^[67] first demonstrated this principle by assembling MV-functionalized polymeric nanoparticles around an Azo-modified silica core via heteroternary complexation (MV@CB[8]@Azo, Type II, Figure 2B). The resulting structures featured a hierarchical “raspberry” configuration, confirmed by electron microscopy, and showcased dynamic photocontrol (Figure 7A). UV-induced *trans*-to-*cis* isomerization of Azo disrupted the host–guest complexes and temporarily disassembled the colloids; exposure to visible light reversed the isomerization and reassembled the raspberry-like structures. This study laid the foundation for employing CB[n] macrocycles in light-responsive colloidal systems with switchable morphologies.

Subsequent research expanded on these concepts by leveraging the dual functionality of CB[n] to stabilize and organize metal nanoparticles on polymer colloids, thereby creating robust nanocomposites for catalysis. Wu et al.^[34] incorporated CB[7] onto MV-functionalized polymeric spheres (CB[n]@MV 1:1), then anchored palladium (Pd) nanoparticles to the CB[7] portal sites (Type V, Figure 2E), forming stable, uniform raspberry-like architectures with high catalytic activity for Suzuki coupling reactions (Figure 7C). Beyond Pd, this platform proved versatile for other metals like gold and silver, underlining the broad utility of CB[7] in suppressing nanoparticle aggregation and thereby preserving catalytic performance over multiple reaction cycles.

Pushing these approaches further, Hu et al.^[68] introduced paramagnetic iron oxide nanoparticles into the corona and demonstrated that the same CB[8]-based heteroternary complexation (MV@CB[8]@Azo, Type II, Figure 2B) could impart photoresponsive assembly and disassembly, enabling controlled release of the entrapped cargo (Figure 7B). They also investigated the rheological properties of these dispersions, showing that the raspberry-like colloids could reversibly switch between shear-thickening and shear-thinning states under different light exposures. Such dual physical responsiveness, including magnetic manipulation and photo-switchable assembly, highlights the enormous design flexibility afforded by CB[n] host–guest interactions in next-generation colloidal systems. Building on this concept, Hu et al.^[69] further investigated the photocontrolled rheological behavior of colloidal dispersions with CB[8]. By assembling MV-functionalized iron oxide nanoparticles onto an Azo-functionalized silica core, they created hybrid raspberry-like colloids (Figure 7D), which also formed heteroternary complexes of MV@CB[8]@Azo 1:1:1 (Type II, Figure 2B). This assembly enabled the colloids to exhibit reversible photocontrolled behavior, switching between shear-thickening and shear-thinning states upon light exposure.

These studies emphasize how CB[n]-mediated chemistry underpins the formation of raspberry-like colloids that are both structurally complex and functionally versatile. By integrating magnetic, catalytic, and photoresponsive behaviors into a single core–corona architecture, researchers are forging new paths for stimuli-responsive materials with broad potential in advanced coatings, drug delivery, smart fluids, and beyond.

2.4. Core–Shell Colloidal Superstructures

Core–shell colloids are sophisticated colloidal structures composed of a central core particle encased within a shell of a different material.^[7] These colloids, typically ranging from the nanometer to micrometer scale, are defined by distinct layering achieved through various interparticle interactions. The materials for the core and shell can be independently tailored, allowing a wide range of physical and chemical properties within a single colloidal entity. This structural design offers unique advantages in applications requiring specific surface characteristics, optical properties, or chemical stability.^[70] For instance, the core can provide mechanical strength or magnetic properties, while the shell can offer protection, biocompatibility, or catalytic activity.^[7] Core–shell colloids have applications in various fields, including drug delivery, where they facilitate controlled release and targeted delivery of therapeutic agents,^[71] and catalysis, where the shell can act as a selective barrier or catalytic surface.^[72] Additionally, they are used in electronics and optics, where the core–shell structure enhances electrical conductivity or light absorption.^[73] The synthesis of core–shell colloids can be accomplished through various methods, such as sol-gel processes,^[9] emulsion polymerization,^[10] and layer-by-layer deposition,^[74] which allow precise control over the thickness and composition to suit specific applications.

An early demonstration of this dynamic control harnessed CB[8] host–guest interactions as a “molecular handcuff” to assemble cleavable core–shell microspheres. Lan et al.^[75] en-

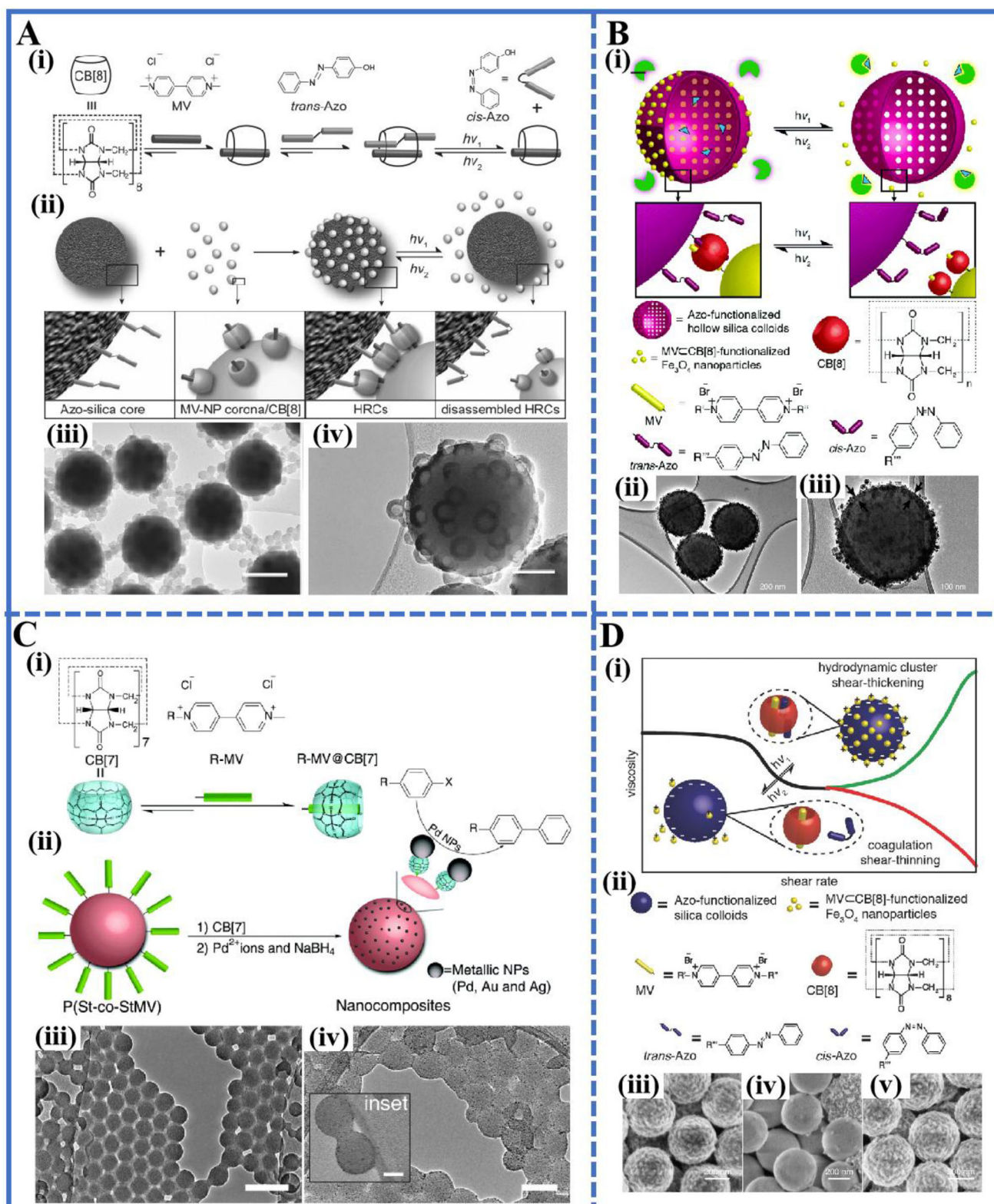


Figure 7. A) i) Stepwise formation of heteroternary complex of MV@CB[8]@Azo 1:1:1 and light-driven reversible disassembly of the complex. ii) Raspberry-like colloids obtained by the formation of heteroternary complex and light-driven reversible disassembly. TEM images of SiO₂-coated raspberry-like colloids (iii, scale bars, 200 nm) before and (iv, scale bars, 100 nm) after calcination.^[67] Reproduced with permission from ref. [67] copyright 2014, Wiley-VCH. B) i) Hybrid multi-component raspberry-like colloids (HMRCs) obtained through the formation of heteroternary complexes of MV@CB[8]@Azo 1:1:1 and the light-driven reversible disassembly of the HMRCs. ii, iii) TEM image of the HMRC.^[68] Reproduced with permission

gineered polymeric cores and acylate-based shell polymers functionalized with complementary guest moieties, MV and Np, which selectively bind inside the CB[8] cavity (**Figure 8A**). This arrangement yields a robust heteroternary complex (MV@CB[8]@Np, Type II, **Figure 2B**) that envelops the core with a functional shell, yet it remains reversible under mild conditions. Introducing a competing guest (ADA) displaces the MV–Np pair and triggers shell detachment, showcasing a supramolecular on/off mechanism. In biomedical contexts, such switchable core–shell architectures hold immense promise for stimuli-responsive drug release and therapies that demand controlled activation or deactivation within biological environments.

Building on the versatility of CB[8] in constructing dynamic and reversible supramolecular systems, Zhu et al.^[76] extended the concept to immuno-affinity supramolecular magnetic nanoparticles (ISM-NPs) for the efficient capture and gentle release of small extracellular vesicles (sEVs). By bridging antibodies onto magnetic cores via CB[8]-mediated heteroternary complexes (e.g., Np and bipyridine guests, Type IV, **Figure 2D**), they fashioned cleavable linkages that minimize damage to sEVs during isolation and re-collection (**Figure 8B**). This design achieved both high capture (85.5%) and release (>82%) efficiencies, preserving the vesicles' structure and offering new capabilities in diagnostics and therapeutic development. The reversibility of the CB[8]-based linkages under mild conditions underscores the potential for fine-tuned control in future bioseparation and purification platforms.

The selective host–guest chemistry of CB[n] also opens opportunities in catalysis and biosensing. Mao et al.^[77] revealed that CB[6] can selectively bind certain substrates, such as 2,2'-biazobis(3-ethylbenzothiazoline-6-sulfonic acid) (ABTS), to catalyze reactions effectively. By coating oxidase-loaded zeolitic imidazolate framework-8 (ZIF-8) with CB[6] (CB[6]/GOx@ZIF-8, Type V, **Figure 2E**), the authors created a unique supramolecule/biomolecule@nanomaterial core–shell architecture (**Figure 8C**). This design retained CB[6]'s catalytic selectivity while leveraging a cascade reaction pathway to boost signal detection of glucose and cholesterol. The synergy between the macrocyclic host and the ZIF-8 framework thus facilitated a sensitive platform for biomarker analysis, illustrating how integrating CB[n] with porous or enzymatic components can elevate functional performance in biosensing.

These studies highlight the transformative role of CB[n]-based chemistry in elevating core–shell colloids from static composites to dynamic, interactive nanoplatfroms. By enabling reversible shell formation, selective molecular capture and release, and tunable catalytic activity, CB[n]s offer unprecedented precision for designing next-generation colloidal systems. These advances

promise wide-ranging applications, from targeted drug delivery and regenerative medicine to environmental monitoring and advanced nanoelectronics, underscoring the versatility and power of supramolecular strategies in shaping the future of functional materials.

2.5. Colloidosomes

Colloidosomes represent a distinct category of microcapsules with a shell composed of colloidal particles enclosing a hollow interior.^[8] These particles can be made from various materials, such as polymers, metals, or silica, while the hollow space within colloidosomes is adept at encapsulating diverse substances, including pharmaceuticals, genetic material, proteins, and imaging agents. The precise control over size, shape, and constituent materials allows for fine-tuning of their physicochemical properties, enabling controlled release behaviors that are particularly useful in biomedical applications.^[78] However, traditional methods for preparing colloidosomes, such as emulsion polymerization, electrospray, acoustic-based techniques, and template-assisted self-assembly, present challenges. These include complex purification processes, batch-to-batch inconsistencies, and limited control over the size, shape, and stability of the final structures.^[79–83] Recent advances in microfluidics technologies, particularly have revolutionized colloidosome fabrication. Microfluidic platforms, particularly droplet-based systems, have addressed many of these limitations. These systems generate microdroplets with precise sizes, which can then be stabilized to form colloidosomes with enhanced monodispersity and functionality.

Recent work has leveraged CB[n] host–guest chemistry to enhance both the precision and responsiveness of colloidosome shells. In a pioneering example, Zhang et al.^[79] employed a one-step microfluidic strategy in which MV-functionalized AuNPs and Np-functionalized polymers formed heteroternary complexes with CB[8] (Type II, **Figure 2B**), self-assembling into robust shells at droplet interfaces (**Figure 9A**). This process not only yielded highly monodisperse colloidosomes but also enabled encapsulation of diverse cargo (e.g., fluorescein isothiocyanate-dextran (FD), rhodamine B) and facilitated controlled release through the redox-triggered disruption of MV@CB[8]@Np complexes. Notably, the presence of AuNPs imparted SERS capabilities, illustrating how colloidosomes can be functionalized for both cargo delivery and in situ sensing.

Building on these concepts, Stephenson et al.^[84] demonstrated a similar microfluidic assembly approach, employing polystyrene nanoparticles bearing MV groups crosslinked by CB[8] and a Np-functionalized polyacrylamide linker (**Figure 9B**). The evaporation of the continuous phase induced tight packing of the nanoparticles into hollow shells, again stabilized by CB[8]-

from ref. [68] copyright 2016, The Royal Society of Chemistry. C) i) Complexation between MV and CB[7]. ii) Schematic representation of the formation of polymeric nanocomposites through in situ reduction of metallic ions in an aqueous suspension of the P(St-co-StMV)/CB[7]. TEM images of iii) P(St-co-StMV) colloids (scale bars: 100 nm) and iv) Pd@P(St-co-StMV) nanocomposites (scale bars, 50 nm. Inset scale bars: 20 nm).^[34] Reproduced with permission from ref. [34] copyright 2015, The Royal Society of Chemistry. D) i) Schematic of the rheological behavior in the light-induced reversible assembly of raspberry-like colloids. ii) Functional components used to assemble hybrid raspberry colloids, with CB[8] as a supramolecular linker. SEM images of iii) assembled raspberry-like colloids; iv) disassembled raspberry-like colloids, and v) reassembled raspberry-like colloids.^[69] Reproduced with permission from ref. [69] copyright 2018, Wiley-VCH.

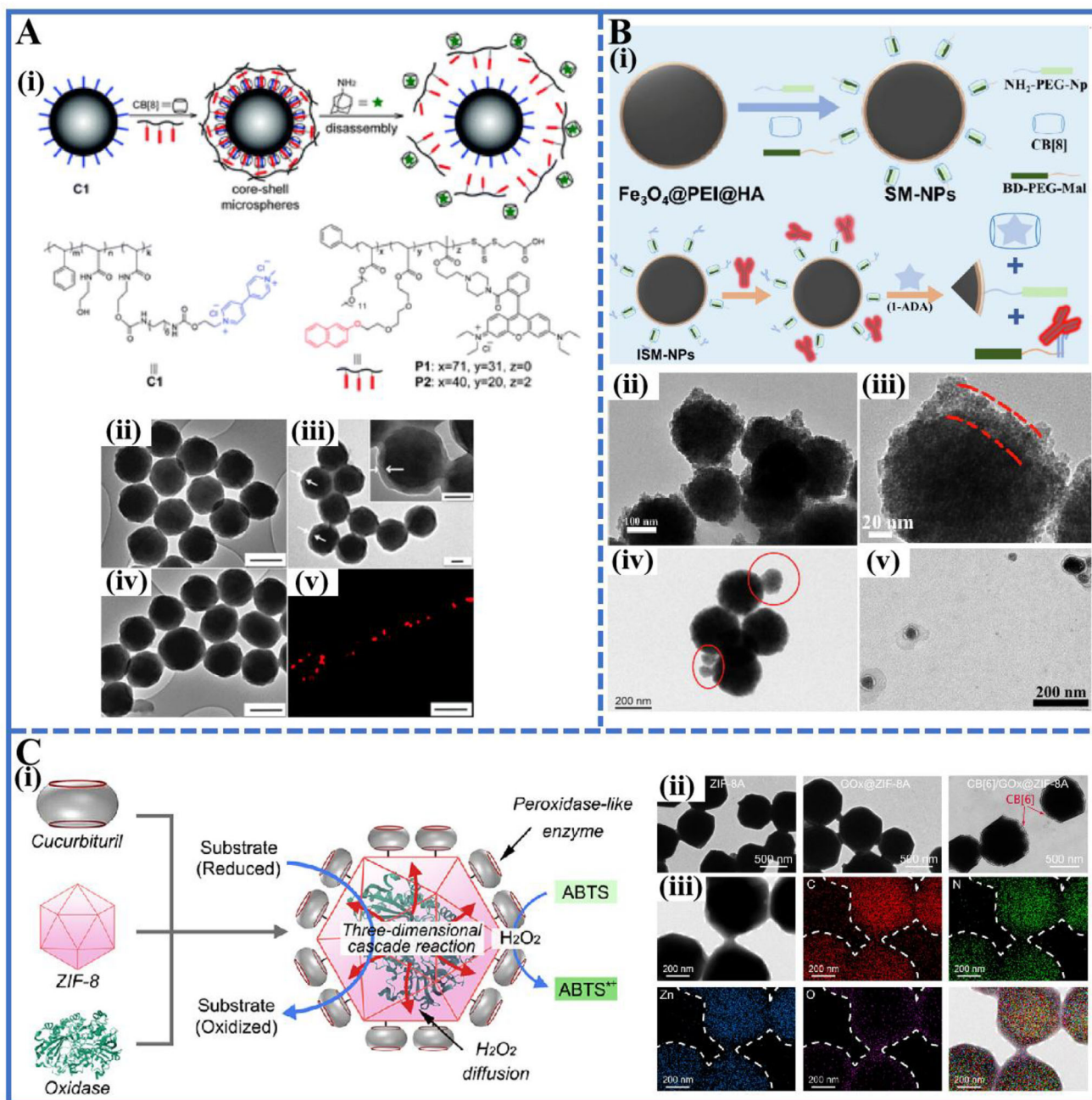


Figure 8. A) i) Reversible preparation of core-shell polymeric microspheres via the formation and dissociation of a heteroternary complex of MV@CB[8]@Azo 1:1:1. TEM images show ii) C1, iii) core-shell polymeric microspheres, and iv) the disassembled microspheres. v) CLSM image of the core-shell microspheres. Scale bars: ii, iv) 200 nm, iii) 100 nm, v) 5 nm.^[75] Reproduced with permission from ref. [75] copyright 2012, The Royal Society of Chemistry. B) i) The schematic illustration of ISM-NPs assembly and disassembly in the presence of 1-ADA. TEM images show ii) ISM-NPs, iv) small extracellular vesicles (sEVs) captured by ISM-NPs, and v) release of sEVs from the ISM-NP-sEV complex. Scale bars are as follows: ii) 100 nm, iii) 20 nm, iv, v) 200 nm.^[76] Reproduced with permission from ref. [76] copyright 2022, Elsevier Ltd. Additionally, C) i) presents a schematic of the synthesis process for the CB[6]/Ox@ZIF-8A nanocomposite. ii) TEM images of ZIF-8A, GOx@ZIF-8A, and CB[6]/GOx@ZIF-8A. Scale bars: 500 nm. iii) Transmission electron microscopy–energy dispersive spectroscopy (TEM-EDS) mapping images of the GOx/CB[6]@ZIF-8A nanocomposite.^[77] Reproduced with permission from ref. [77] copyright 2021, American Chemical Society.

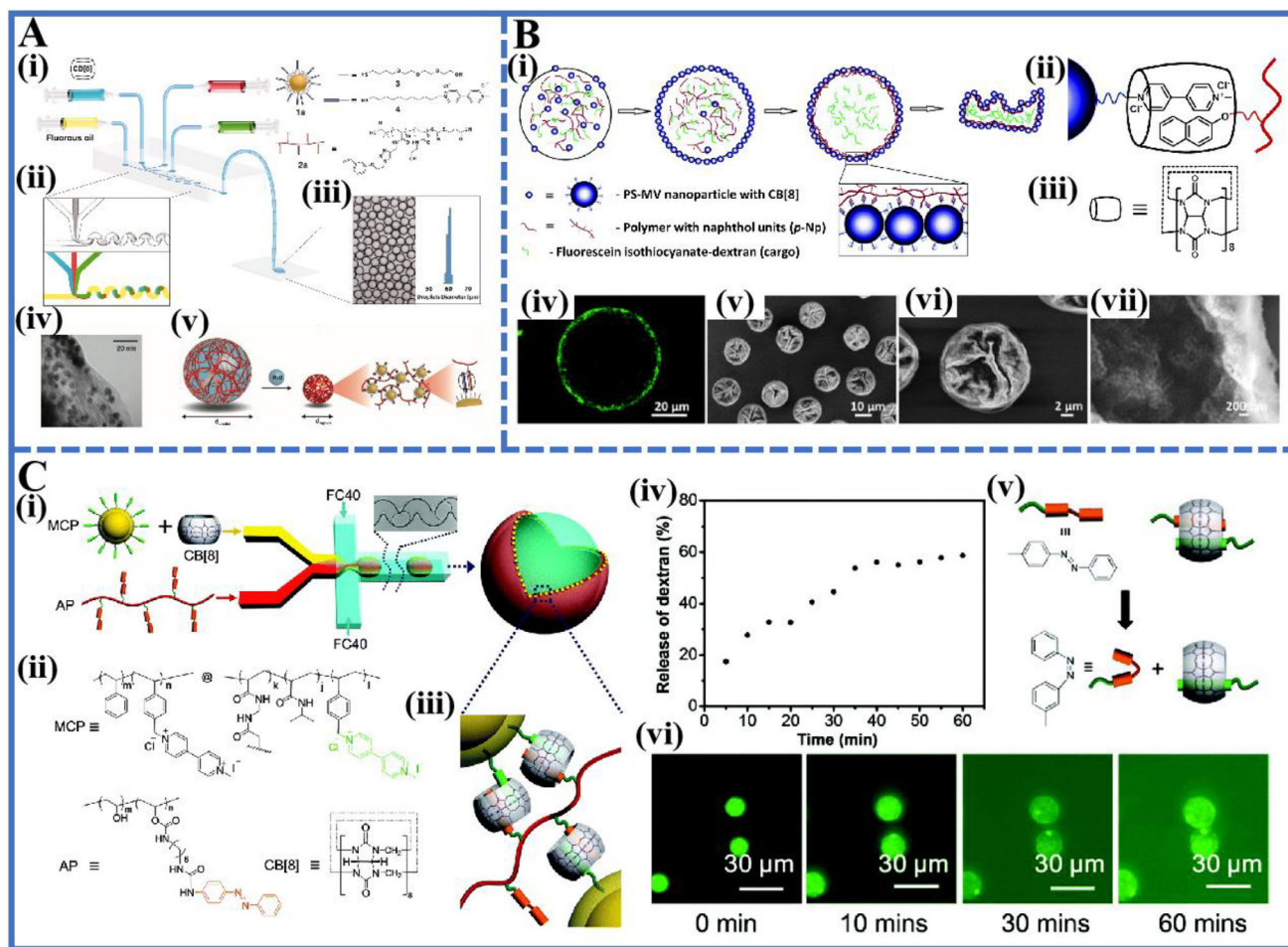


Figure 9. A) i, ii) Schematic representation of the microdroplet generation process using a microfluidic T-junction device. iii) The high monodispersity of microfluidic droplets is demonstrated. iv) TEM image of the microcapsule shell, showing AuNPs ≈ 5 nm in diameter. v) Schematic representation of the proposed microcapsule formation process.^[79] Reproduced with permission from ref. [79] copyright 2012, American Association for the Advancement of Science. B) i) Schematic of colloidosome formation. ii) Schematic of the ternary supramolecular complex formed. iii) The molecular structure of CB[8]. iv–vii) The colloidosome formed from the interfacial assembly of PS-MV, CB[8] and p-Np.^[84] Reproduced with permission from ref. [84] copyright 2014, The Royal Society of Chemistry. C) i) Schematic of the preparation of supramolecular colloidal microcapsules by a flow-focusing microfluidic device. ii) Molecular structure of MCP, AP, and CB[8]. iii) Schematic representation of the proposed microcapsule from CB[8]-mediated supramolecular assembly. iv) The release profile of 150 kDa FD cargo from microcapsules over 1 h after 30 s of UV irradiation at 377 nm. v) Schematic representation of the photochemical disassembly of the heteroternary complex between MV, Azo, and CB[8]. vi) Fluorescence images showing the triggered release of 150 kDa FD cargo from microcapsules, upon exposure to UV light.^[85] Reproduced with permission from ref. [85] copyright 2016, The Royal Society of Chemistry.

mediated heteroternary complexes. This approach further underscored the versatility of colloidosomes for cargo encapsulation and controlled release, reinforcing the promise of supramolecular host–guest interactions in creating stable yet reconfigurable microcapsules.

More recently, attention has turned to introducing multiple stimuli-responsive properties within a single colloidosome system. Yu et al.^[85] incorporated both thermal and photoresponsive components by combining poly(*N*-isopropylacrylamide) (PNIPAM) and Azo moieties into the colloidosome shell (Figure 9C). These colloidosomes were formed by combining MV-bearing colloidal particles (MCPs) and an Azo-functionalized polymer (AP) within microfluidic droplets. Upon the addition of CB[8] in the microfluidic device, heteroternary complexation of

MV@CB[8]@Azo 1:1:1 occurs at the droplet interface (Type II, Figure 2B). Above its lower critical solution temperature (LCST), the PNIPAM component undergoes a conformational shift that increases shell permeability, enabling thermo-triggered cargo release. Simultaneously, UV-induced Azo isomerization breaks the supramolecular crosslinks (MV@CB[8]@Azo), offering an additional light-responsive release mechanism. This dual-stimulus approach showcases the powerful synergy between microfluidic precision and CB[8]-mediated complexation, paving the way for the design of “smart” colloidosomes that respond to multiple external cues.

These studies illustrate a rapid evolution in colloidosome technology, progressing from simpler microcapsules to highly sophisticated, multifunctional constructs. By inte-

Table 1. Different strategies for CB[n]-mediated colloidal superstructures.

Colloidal structure	Key structural features	Advantages	Applications	Limitations
Colloidal Clusters	<ul style="list-style-type: none"> Controlled interparticle gaps (0.91 nm) 	<ul style="list-style-type: none"> Sub-nanometer precision Enhanced plasmonic coupling Tunable optical properties 	<ul style="list-style-type: none"> SERS sensing Catalysis Photothermal therapy 	<ul style="list-style-type: none"> Limited to metal NPs due to electrostatic forces
1D Colloidal Chains	<ul style="list-style-type: none"> End-to-end aligned NPs/nanorods Programmable junctions 	<ul style="list-style-type: none"> Anisotropic properties Stimuli-responsive reconfiguration Dynamic assembly/disassembly 	<ul style="list-style-type: none"> Nanowire electronics Optical waveguides Mechanically responsive sensors 	<ul style="list-style-type: none"> Requires end-specific functionalization Scalability challenges
Raspberry-Like Colloids	<ul style="list-style-type: none"> Core–corona hierarchy Hybrid structures (polymer/magnetic/NP) Reversible assembly 	<ul style="list-style-type: none"> Multifunctional surfaces High surface area Responsive to external stimuli 	<ul style="list-style-type: none"> Targeted drug delivery Catalytic reactors Tunable rheological fluids 	<ul style="list-style-type: none"> Complex synthesis steps Potential corona inhomogeneity
Core–Shell Colloids	<ul style="list-style-type: none"> Dynamic shell layers Responsive interfaces Selective molecular recognition 	<ul style="list-style-type: none"> Controlled cargo encapsulation/release Selective molecular recognition Tunable catalytic activity 	<ul style="list-style-type: none"> Biomedical carriers Bioseparation Enzyme-mimetic catalysis 	<ul style="list-style-type: none"> Dual guest functionalization required Competitive guest interference
Colloidosomes	<ul style="list-style-type: none"> Hollow microcapsules Nanoparticle-stabilized shells Modular cargo loading 	<ul style="list-style-type: none"> High monodispersity Multi-stimuli responsiveness Customizable release profiles 	<ul style="list-style-type: none"> Encapsulated drug delivery Diagnostic probes Microreactors 	<ul style="list-style-type: none"> Specialized fabrication (e.g., microfluidics) Limited shell permeability tuning

grating CB[n]-based host–guest interactions into microfluidic production, researchers have unlocked unprecedented control over colloidosome assembly and properties. This, in turn, opens wide-ranging possibilities in areas such as drug delivery, diagnostics, and advanced materials, where customizable release profiles and stimuli-responsive behavior are paramount.

As demonstrated in **Table 1**, the comparative analysis outlines the key features, applications, advantages, and limitations of various CB[n]-mediated self-assembly strategies, providing a concise reference to facilitate comparison across systems.

3. Conclusion and Perspectives

In this review, we have explored the transformative role of cucurbit[n]urils (CB[n]) in colloidal science, highlighting their capacity to mediate the assembly of colloidal particles into sophisticated architectures, ranging from colloidal clusters and 1D chains to raspberry-like assemblies, core–shell colloids, and colloidosomes. The unique host–guest chemistry of CB[n] not only imparts exceptional stability and responsiveness to these systems but also enables a wide range of functions, facilitating applications in catalysis, drug delivery, sensing, and beyond. Leveraging diverse synthetic strategies has further allowed researchers to fine-tune parameters such as particle size, composition, and assembly dynamics. Moreover, CB[n]’s intrinsic ability to encapsulate and protect guest molecules extends the performance and lifetime of colloidal structures.

Overall, CB[n]-mediated colloidal assemblies represent a promising avenue for a variety of advanced applications. However, several challenges and limitations must be addressed to fully unlock their potential: i) Stability under physiological conditions: CB[n]-based assemblies may be sensitive to environmental factors such as pH, ionic strength, and the charge of

the guest molecules. These conditions, often encountered in biological environments, can lead to unexpected aggregation or destabilization.^[86,87] Although CB[n]s themselves are chemically stable, the long-term in vivo stability and biodegradability of CB[n]-mediated colloids require further investigation to ensure safety and efficacy; ii) Scalability and repeatability: The complex and often costly synthesis of CB[n]-mediated colloids pose challenges for large-scale production. Ensuring reproducibility and minimizing batch-to-batch variability are essential for applications like drug delivery and diagnostics, where precise control over assembly properties is essential; iii) Limited functionalization of CB[n]s: Compared to other supramolecular hosts, CB[n]s offer relatively fewer options for chemical modification, which may limit their versatility in interacting with a broader range of guest molecules.

Looking ahead, CB[n]-mediated self-assembly in colloidal science holds significant potential for groundbreaking advancements in materials design and functionality. Several potential directions for future research are outlined below:

3.1. Development of Functionalized CB[n]s for Covalent Attachment to Colloids

Functionalizing CB[n]s to enable covalent bonding to colloidal surfaces signifies a pivotal advancement in colloidal science.^[88] By creating CB[n] derivatives that can be chemically tethered to colloids, researchers could achieve more stable and robust colloidal assemblies. This would facilitate the construction of highly complex and architecturally sophisticated colloidal structures with enhanced durability and functional properties.^[89] Such advancements could enable the design of colloidal systems with applications in targeted drug delivery, environmental sensing, and nanocatalysis.^[90]

3.2. Integration with Emerging Technologies

Integrating CB[n]-mediated colloidal systems with emerging fabrication technologies, such as microfluidics, 3D printing, and soft robotics, presents exciting opportunities.

- i. Microfluidics offers precise control over colloidal assembly processes, allowing for the scalable production of uniform colloidal structures. The responsive nature of CB[n] host-guest interactions allows for the dynamic disassembly of microcapsules under external stimuli, enabling targeted payload release.^[91] This integration highlights the potential of flow-directed colloidal assembly in creating multifunctional materials.
- ii. 3D printing technologies have expanded the possibilities for constructing complex colloidal architectures. Integrating CB[n] host-guest chemistry into 3D bioprinting processes facilitates the fabrication of multilayered tissue constructs with high stability and specificity, advancing tissue engineering.^[92] Additionally, CB[7] has been utilized to fabricate novel photoinitiators such as 3,6-Bis[2-(1-methylpyridinium)vinyl]-9-methyl-carbazole diiodide (BMVMC) to improve the water solubility of 3D hydrogel structure. This development offers promising opportunities for constructing biocompatible 3D hydrogel scaffolds essential for regenerative medicine applications.^[93] In the realm of soft robotics, CB[n]-based supramolecular networks offer materials with adaptive and self-healing properties. These materials exhibit exceptional stretchability and mechanical resilience, making them ideal for wearable electronics and sensor applications.^[94]
- iii. The convergence of CB[n] chemistry with cutting-edge manufacturing technologies is poised to drive innovation in smart material design, significantly enhancing the functional capabilities of colloidal systems. This opens new pathways to address challenges in personalized medicine, adaptive robotics, and sustainable material development.

3.3. Creation of Responsive and Adaptive Materials

The dynamic and reversible nature of CB[n]-mediated host-guest interactions presents a distinctive advantage for developing responsive and adaptive colloidal materials. Future research could focus on the design of multi-stimuli responsive systems capable of controlled assembly and disassembly in response to environmental triggers such as light, temperature, pH, or specific chemical signals.^[95] These responsive materials hold significant potential for applications in drug delivery, where controlled release is critical, as well as in reconfigurable materials for soft robotics and adaptive optics.

3.4. Multi-Functional Assemblies and Hybrid Materials

The future of CB[n]-mediated self-assembly may also lie in the synthesis of hybrid colloidal materials that combine the unique properties of CB[n]s with other nanomaterials or supramolecular systems. For example, the integration of CB[n] chemistry with

metal-organic frameworks, graphene, or other functional nanomaterials could yield multi-functional assemblies with enhanced mechanical, electrical, or catalytic properties.^[96–98] These hybrid systems could find application across diverse fields, including energy storage, environmental remediation, and advanced sensing technologies.

In conclusion, CB[n]-mediated colloidal science has matured into a versatile, dynamic field, poised to shape the next generation of functional materials. By capitalizing on CB[n]'s precise binding, robust stability, and adaptability, researchers are well-positioned to develop innovative solutions to existing challenges and to pioneer entirely new applications across diverse scientific and technological domains.

Acknowledgements

H.X., C.G., and S.Z. contributed equally to this work. Y.Z. acknowledges the support of the National Natural Science Foundation of China (Grant No. 22204065).

Conflict of Interest

The authors declare no conflict of interest.

Keywords

colloidal superstructures, cucurbit[n]urils, high precision, host-guest interactions, self-assemblies

Received: February 26, 2025

Revised: April 18, 2025

Published online:

- [1] S.-H. Kim, J.-M. Lim, S.-K. Lee, C.-J. Heo, S.-M. Yang, *Soft Matter* **2010**, 6, 1092.
- [2] Y. Chen, P. Xu, M. Wu, Q. Meng, H. Chen, Z. Shu, J. Wang, L. Zhang, Y. Li, J. Shi, *Adv. Mater.* **2014**, 26, 4294.
- [3] E. C. Montoto, G. Nagarjuna, J. Hui, M. Burgess, N. M. Sekerak, K. Hernández-Burgos, T.-S. Wei, M. Kneer, J. Grolman, K. J. Cheng, J. A. Lewis, J. S. Moore, J. Rodríguez-López, *J. Am. Chem. Soc.* **2016**, 138, 13230.
- [4] A. van Blaaderen, *Science* **2003**, 301, 470.
- [5] Y. Xia, P. Yang, Y. Sun, Y. Wu, B. Mayers, B. Gates, Y. Yin, F. Kim, H. Yan, *Adv. Mater.* **2003**, 15, 353.
- [6] Y. Lan, A. Caciagli, G. Guidetti, Z. Yu, J. Liu, V. E. Johansen, M. Kamp, C. Abell, S. Vignolini, O. A. Scherman, E. Eiser, *Nat. Commun.* **2018**, 9, 3614.
- [7] D. He, C. Zhang, G. Zeng, Y. Yang, D. Huang, L. Wang, H. Wang, *Appl. Catal. B* **2019**, 258, 117957.
- [8] A. D. Dinsmore, M. F. Hsu, M. G. Nikolaides, M. Marquez, A. R. Bausch, D. A. Weitz, *Science* **2002**, 298, 1006.
- [9] W. Stöber, A. Fink, E. Bohn, *J. Colloid Interface Sci.* **1968**, 26, 62.
- [10] A. SarÄ, C. Alkan, A. Biçer, A. Altuntaş, C. Bilgin, *Energy Convers. Manage.* **2014**, 86, 614.
- [11] A. Zhu, A. Cai, Z. Yu, W. Zhou, *J. Colloid Interface Sci.* **2008**, 322, 51.
- [12] D. Qi, Y. Bao, Z. Weng, Z. Huang, *Polymer* **2006**, 47, 4622.
- [13] Y. Ye, X. Zeng, H. Li, P. Chen, C. Ye, F. Zhao, *J. Macromol. Sci. Part A* **2010**, 48, 42.

- [14] F. Zhang, C. Yu, *J. Macromol. Sci. Part A* **2007**, 44, 559.
- [15] Y. Wang, Y. Li, R. Zhang, L. Huang, W. He, *Polym. Compos.* **2006**, 27, 282.
- [16] K. Richter, A. Birkner, A.-V. Mudring, *Angew. Chem., Int. Ed.* **2010**, 49, 2431.
- [17] A. Shavel, L. Guerrini, R. A. Alvarez-Puebla, *Nanoscale* **2017**, 9, 8157.
- [18] R. J. Archer, A. J. Parnell, A. I. Campbell, J. R. Howse, S. J. Ebbens, *Adv. Sci.* **2018**, 5, 1700528.
- [19] D. Li, L. Qi, *Curr. Opin. Colloid Interface Sci.* **2018**, 35, 59.
- [20] S. J. Barrow, S. Kasera, M. J. Rowland, J. del Barrio, O. A. Scherman, *Chem. Rev.* **2015**, 115, 12320.
- [21] W. A. Freeman, W. L. Mock, N. Y. Shih, *J. Am. Chem. Soc.* **1981**, 103, 7367.
- [22] J. Kim, I.-S. Jung, S.-Y. Kim, E. Lee, J.-K. Kang, S. Sakamoto, K. Yamaguchi, K. Kim, *J. Am. Chem. Soc.* **2000**, 122, 540.
- [23] W.-H. Huang, S. Liu, P. Y. Zavalij, L. Isaacs, *J. Am. Chem. Soc.* **2006**, 128, 14744.
- [24] S. R. Peerannawar, V. V. Gobre, S. P. Gejji, *Comput. Theor. Chem.* **2011**, 966, 154.
- [25] Q. Li, S.-C. Qiu, J. Zhang, K. Chen, Y. Huang, X. Xiao, Y. Zhang, F. Li, Y.-Q. Zhang, S.-F. Xue, Q.-J. Zhu, Z. Tao, L. F. Lindoy, G. Wei, *Org. Lett.* **2016**, 18, 4020.
- [26] F. Biedermann, O. A. Scherman, *J. Phys. Chem. B* **2012**, 116, 2842.
- [27] S. Mecozzi, J. Rebek Jr., *Chem.-Eur. J.* **1998**, 4, 1016.
- [28] K. I. Assaf, W. M. Nau, *Chem. Soc. Rev.* **2014**, 44, 394.
- [29] D. Shetty, J. K. Khedkar, K. M. Park, K. Kim, *Chem. Soc. Rev.* **2015**, 44, 8747.
- [30] K. Jansen, H.-J. Buschmann, A. Wego, D. Döpp, C. Mayer, H.-J. Drexler, H.-J. Holdt, E. Schollmeyer, *J. Inclusion Phenom. Macrocyclic Chem.* **2001**, 39, 357.
- [31] H.-J. Buschmann, E. Cleve, K. Jansen, A. Wego, E. Schollmeyer, *J. Inclusion Phenom. Macrocyclic Chem.* **2001**, 40, 117.
- [32] Y. Miyahara, K. Abe, T. Inazu, *Angew. Chem., Int. Ed.* **2002**, 41, 3020.
- [33] W. L. Mock, N. Y. Shih, *J. Org. Chem.* **1983**, 48, 3618.
- [34] Y. Wu, Y. Lan, J. Liu, O. A. Scherman, *Nanoscale* **2015**, 7, 13416.
- [35] W. S. Jeon, K. Moon, S. H. Park, H. Chun, Y. H. Ko, J. Y. Lee, E. S. Lee, S. Samal, N. Selvapalam, M. V. Rekharsky, V. Sindelar, D. Sobransingh, Y. Inoue, A. E. Kaifer, K. Kim, *J. Am. Chem. Soc.* **2005**, 127, 12984.
- [36] H.-J. Kim, J. Heo, W. S. Jeon, E. Lee, J. Kim, S. Sakamoto, K. Yamaguchi, K. Kim, *Angew. Chem., Int. Ed.* **2001**, 40, 1526.
- [37] G. Wu, M. Olesińska, Y. Wu, D. Matak-Vinkovic, O. A. Scherman, *J. Am. Chem. Soc.* **2017**, 139, 3202.
- [38] B. Ambrose, G. Sathiyaraj, M. Kathiresan, *Sci. Rep.* **2024**, 14, 5786.
- [39] R. J. Coulston, S. T. Jones, T.-C. Lee, E. A. Appel, O. A. Scherman, *Chem. Commun.* **2010**, 47, 164.
- [40] L. Isaacs, *Chem. Commun.* **2009**, 2009, 619.
- [41] X.-L. Ni, X. Xiao, H. Cong, Q.-J. Zhu, S.-F. Xue, Z. Tao, *Acc. Chem. Res.* **2014**, 47, 1386.
- [42] J. Lagona, P. Mukhopadhyay, S. Chakrabarti, L. Isaacs, *Angew. Chem., Int. Ed.* **2005**, 44, 4844.
- [43] T.-C. Lee, O. A. Scherman, *Chem. Commun.* **2010**, 46, 2438.
- [44] S. T. Jones, J. M. Zayed, O. A. Scherman, *Nanoscale* **2013**, 5, 5299.
- [45] Y. Xu, X. Wang, X. Ma, *Dyes Pigm.* **2017**, 145, 385.
- [46] F. Benyetou, X. Zheng, E. Elacqua, Y. Wang, P. Dalvand, Z. Asfari, J.-C. Olsen, D. S. Han, N. Saleh, M. Elhabiri, M. Weck, A. Trabolzi, *Langmuir* **2016**, 32, 7144.
- [47] Y.-J. Kim, J.-H. Kim, I.-S. Jo, D. J. Pine, S. Sacanna, G.-R. Yi, *J. Am. Chem. Soc.* **2021**, 143, 13175.
- [48] Y.-J. Kim, J.-B. Moon, H. Hwang, Y. S. Kim, G.-R. Yi, *Adv. Mater.* **2023**, 35, 2203045.
- [49] X. Meng, H. Wu, M. Morbidelli, *Langmuir* **2015**, 31, 1113.
- [50] S. Ravaine, E. Duguet, *Curr. Opin. Colloid Interface Sci.* **2017**, 30, 45.
- [51] É. Ducrot, M. He, G.-R. Yi, D. J. Pine, *Nat. Mater.* **2017**, 16, 652.
- [52] Y. Liu, J. Wang, I. Imaz, D. Maspoch, *J. Am. Chem. Soc.* **2021**, 143, 12943.
- [53] R. W. Taylor, T.-C. Lee, O. A. Scherman, R. Esteban, J. Aizpurua, F. M. Huang, J. J. Baumberg, S. Mahajan, *ACS Nano* **2011**, 5, 3878.
- [54] Y. Teng, X. Li, Y. Chen, P. Xu, Z. Pan, K. Shao, N. Sun, *Microchim. Acta* **2023**, 190, 185.
- [55] G. Davison, T. Jones, J. Liu, J. Kim, Y. Yin, D. Kim, W.-I. K. Chio, I. P. Parkin, H.-H. Jeong, T.-C. Lee, *Adv. Mater. Technol.* **2023**, 8, 2201400.
- [56] X. Xu, F. Tian, X. Liu, R. M. Parker, Y. Lan, Y. Wu, Z. Yu, O. A. Scherman, C. Abell, *Chem.-Eur. J.* **2015**, 21, 15516.
- [57] S.-Y. Zhang, M. D. Regulacio, M.-Y. Han, *Chem. Soc. Rev.* **2014**, 43, 2301.
- [58] F. Patolsky, C. M. Lieber, *Mater. Today* **2005**, 8, 20.
- [59] Y. Li, F. Qian, J. Xiang, C. M. Lieber, *Mater. Today* **2006**, 9, 18.
- [60] A. N. Generalova, V. A. Oleinikov, E. V. Khaydukov, *Adv. Colloid Interface Sci.* **2021**, 297, 102543.
- [61] N. Hüskens, R. W. Taylor, D. Zigah, J.-C. Taveau, O. Lambert, O. A. Scherman, J. J. Baumberg, A. Kuhn, *Nano Lett.* **2013**, 13, 6016.
- [62] E. Elacqua, X. Zheng, M. Weck, *ACS Macro Lett.* **2017**, 6, 1060.
- [63] L. Zhang, H. Zhang, M. Liu, B. Dong, *ACS Appl. Mater. Interfaces* **2016**, 8, 15654.
- [64] S. S. Acharyya, S. Ghosh, R. Bal, *ACS Appl. Mater. Interfaces* **2014**, 6, 14451.
- [65] Z. Li, Y. Hu, Z. Miao, H. Xu, C. Li, Y. Zhao, Z. Li, M. Chang, Z. Ma, Y. Sun, F. Besenbacher, P. Huang, M. Yu, *Nano Lett.* **2018**, 18, 6778.
- [66] E. Shirman, T. Shirman, A. V. Shneidman, A. Grinthal, K. R. Phillips, H. Whelan, E. Bulger, M. Abramovitch, J. Patil, R. Nevarez, J. Aizenberg, *Adv. Funct. Mater.* **2018**, 28, 1704559.
- [67] Y. Lan, Y. Wu, A. Fox, O. A. Scherman, *Angew. Chem., Int. Ed.* **2014**, 126, 2198.
- [68] C. Hu, K. R. West, O. A. Scherman, *Nanoscale* **2016**, 8, 7840.
- [69] C. Hu, J. Liu, Y. Wu, K. R. West, O. A. Scherman, *Small* **2018**, 14, 1703352.
- [70] R. G. Chaudhuri, S. Paria, *Chem. Rev.* **2012**, 112, 2373.
- [71] Z. Zhang, L. Wang, J. Wang, X. Jiang, X. Li, Z. Hu, Y. Ji, X. Wu, C. Chen, *Adv. Mater.* **2012**, 24, 1418.
- [72] H. She, Y. Sun, S. Li, J. Huang, L. Wang, G. Zhu, Q. Wang, *Appl. Catal. B* **2019**, 245, 439.
- [73] S. Ye, M. Yan, X. Tan, J. Liang, G. Zeng, H. Wu, B. Song, C. Zhou, Y. Yang, H. Wang, *Appl. Catal. B* **2019**, 250, 78.
- [74] R. Shokry, D. Aman, H. M. Abd El Salam, S. Mikhail, T. Zaki, W. M. A. El Roubi, A. A. Farhali, W. Al Zoubi, Y. G. Ko, *Mater. Today Nano* **2024**, 25, 100444.
- [75] Y. Lan, X. J. Loh, J. Geng, Z. Walsh, O. A. Scherman, *Chem. Commun.* **2012**, 48, 8757.
- [76] N. Zhu, Y. Zhang, J. Cheng, Y. Mao, K. Kang, G. Li, Q. Yi, Y. Wu, *J. Colloid Interface Sci.* **2022**, 611, 462.
- [77] D. Mao, W. Li, F. Zhang, S. Yang, A. N. Isak, Y. Song, Y. Guo, S. Cao, R. Zhang, C. Feng, X. Zhu, G. Li, *ACS Appl. Mater. Interfaces* **2021**, 13, 39719.
- [78] H. Jiang, L. Hong, Y. Li, T. Ngai, *Angew. Chem., Int. Ed.* **2018**, 57, 11662.
- [79] J. Zhang, R. J. Coulston, S. T. Jones, J. Geng, O. A. Scherman, C. Abell, *Science* **2012**, 335, 690.
- [80] J. Cui, Y. Wang, A. Postma, J. Hao, L. Hosta-Rigau, F. Caruso, *Adv. Funct. Mater.* **2010**, 20, 1625.
- [81] D. E. Discher, F. Ahmed, *Annu. Rev. Biomed. Eng.* **2006**, 8, 323.
- [82] D. Patra, F. Ozdemir, O. R. Miranda, B. Samanta, A. Sanyal, V. M. Rotello, *Langmuir* **2009**, 25, 13852.
- [83] F. Caruso, R. A. Caruso, H. Möhwald, *Science* **1998**, 282, 1111.
- [84] G. Stephenson, R. M. Parker, Y. Lan, Z. Yu, O. A. Scherman, C. Abell, *Chem. Commun.* **2014**, 50, 7048.
- [85] Z. Yu, Y. Lan, R. M. Parker, W. Zhang, X. Deng, O. A. Scherman, C. Abell, *Polym. Chem.* **2016**, 7, 5996.

- [86] M. Wang, G. Gong, J. Feng, T. Wang, C. Ding, B. Zhou, W. Jiang, J. Fu, *ACS Appl. Mater. Interfaces* **2016**, *8*, 23289.
- [87] X. Lu, E. Masson, *Langmuir* **2011**, *27*, 3051.
- [88] S. K. Ghosh, A. Dhamija, Y. H. Ko, J. An, M. Y. Hur, D. R. Boraste, J. Seo, E. Lee, K. M. Park, K. Kim, *J. Am. Chem. Soc.* **2019**, *141*, 17503.
- [89] C. Sun, Z. Wang, L. Yue, Q. Huang, Q. Cheng, R. Wang, *J. Am. Chem. Soc.* **2020**, *142*, 16523.
- [90] H. Yin, Q. Cheng, D. Bardelang, R. Wang, *JACS Au* **2023**, *3*, 2356.
- [91] Z.-J. Meng, J. Liu, Z. Yu, H. Zhou, X. Deng, C. Abell, O. A. Scherman, *ACS Appl. Mater. Interfaces* **2020**, *12*, 17929.
- [92] J.-H. Shim, K.-M. Jang, S. K. Hahn, J. Y. Park, H. Jung, K. Oh, K. M. Park, J. Yeom, S. H. Park, S. W. Kim, J. H. Wang, K. Kim, D.-W. Cho, *Biofabrication* **2016**, *8*, 014102.
- [93] W. Gao, H. Chao, Y.-C. Zheng, W.-C. Zhang, J. Liu, F. Jin, X.-Z. Dong, Y.-H. Liu, S.-J. Li, M.-L. Zheng, *ACS Appl. Mater. Interfaces* **2021**, *13*, 27796.
- [94] J. Liu, C. S. Y. Tan, Z. Yu, N. Li, C. Abell, O. A. Scherman, *Adv. Mater.* **2017**, *29*, 1605325.
- [95] C. Xu, X. Yu, Y. Liu, X. Zhang, S. Liu, *ACS Appl. Polym. Mater.* **2023**, *5*, 7375.
- [96] J. Liang, A. Nuhnen, S. Millan, H. Breitzke, V. Gvilava, G. Buntkowsky, C. Janiak, *Angew. Chem., Int. Ed.* **2020**, *59*, 6068.
- [97] J. Liang, V. Gvilava, C. Jansen, S. Öztürk, A. Spieß, J. Lin, S. Xing, Y. Sun, H. Wang, C. Janiak, *Angew. Chem., Int. Ed.* **2021**, *60*, 15365.
- [98] D. Xiao, M.-T. Zheng, F.-J. Wu, *Chem. Eng. J.* **2023**, *459*, 141546.



Huimin Xie received her master's degree from Lanzhou University in 2023 and is currently pursuing a Ph.D. at the Photonics Research Institute, Hong Kong Polytechnic University. Her research interests focus on plasmonic nanoparticles, nanophotonics, micro/nano fabrication, and SERS detection.



Chengzhi Guo received his bachelor's degree from Nanjing Tech University in 2022. Currently, he is a Ph.D. candidate at University College London with Dr. Yang Lan. His present research interest focuses on the design and preparation of advanced colloids for gas separation and photocatalytic methane and carbon dioxide conversion.



Shuyu Zhu received her bachelor's degree from Lanzhou University in 2023. She is currently pursuing her master's degree at Lanzhou University under the supervision of Dr. Yuewen Zhang. Her research interests focus on the development of polymer microspheres and raspberry-like plasmonic nanoaggregates and SERS detection.



Yuewen Zhang is a professor at the College of Chemistry and Chemical Engineering, Lanzhou University. She earned her Ph.D. from the Department of Chemistry at the University of Cambridge, followed by postdoctoral research at the National Physical Laboratory and the University of Exeter. She joined Lanzhou University in 2019. Her research focuses on the development of polymer microspheres and raspberry-like plasmonic nanoaggregates, SERS detection, as well as the design of microfluidic devices and their application in biosensing, analysis, and detection.



Yang Lan is an associate professor at University College London. He obtained his Ph.D. from the University of Cambridge (2015) and was a postdoctoral researcher at the University of Cambridge (2015-2017) and the University of Pennsylvania (2017-2019). His research focuses on the interdisciplinary fields of colloids, supramolecular chemistry, and interfaces and the applications in membrane separation and photocatalysis.